Numerical Methods for the Problem of Spurious Oscillations Arising From the Black-Scholes Equation

Zewen Shen

July, 2019

Abstract

The Black-Scholes equation is formally parabolic. However, the numerical approximation behaves as if it was hyperbolic when it is convection dominated. Spurious oscillations appear when a conventional finite difference discretization is applied, leading to approximations that violate the financial rule. While the upwind scheme can eliminate the oscillations, the numerical diffusion it introduced impaired the accuracy of the solution. Thus, we illustrated that the total variation diminishing scheme with flux limiters is one of the best solutions to this problem. In the end, we introduced the discontinuous Galerkin method for further study.

Acknowledgements

I would like to express my deep appreciation to my research project supervisor, Professor Christina Christara, for introducing me to the field of mathematical finance, and also for her patience and guidance during the research. Under her supervision, this research project becomes a valuable learning experience during my undergraduate studies. Finally, I would like to thank my family for their endless support and love.

Contents

1 Introduction

1.1 Black-Scholes equation

For simplification, in this paper, we only consider European put options. The result for call options can be easily replicated by put-call parity.

To model the price evolution of a European option, the famous Black-Scholes equation is proposed by Fischer Black and Myron Scholes in [1], which is in the form:

$$\frac{\partial V}{\partial t} + \frac{1}{2}\sigma^2 S^2 \frac{\partial^2 V}{\partial S^2} + rS\frac{\partial V}{\partial S} - rV = 0, \qquad S \times t \in [0, \infty] \times [0, T], \tag{1.1}$$

or

$$\frac{\partial V}{\partial t} = -\frac{1}{2}\sigma^2 S^2 \frac{\partial^2 V}{\partial S^2} - rS\frac{\partial V}{\partial S} + rV, \qquad S \times t \in [0, \infty] \times [0, T] \tag{1.2}$$

with boundary conditions for European put options

$$V(S, T) = max(E - S, 0), \tag{1.3}$$

$$V(0, t) = Ee^{-r(T-t)}, \tag{1.4}$$

$$V(S,t) \to 0 \;\; as \;\; S \to \infty. \tag{1.5}$$

We need to truncate the domain to make the problem numerically solvable. So (1.2) and (1.5) becomes

$$\frac{\partial V}{\partial t} = -\frac{1}{2}\sigma^2 S^2 \frac{\partial^2 V}{\partial S^2} - rS\frac{\partial V}{\partial S} + rV, \qquad S \times t \in [0, S_{Max}] \times [0, T] \tag{1.6}$$

$$V(S_{Max}, t) = 0. \tag{1.7}$$

Here, V is the price of the put option as a function of stock price S and time t, r is the risk-free interest rate, σ is the volatility of the stock, T is the total time to expiry and E is the strike price.

Notice that the coefficient of $\frac{\partial^2 V}{\partial S^2}$ in (1.2) is a negative number $-\frac{1}{2}\sigma^2 S^2$, which makes the PDE backward parabolic. It turns out that this backward problem is ill-posed: for most initial and boundary conditions, the solution does not exist at all, and even if it does exist, it is likely to blow up within a finite time [2]. Fortunately, we can transform this backward parabolic PDE to a forward parabolic one by the change of variables. Define

$$\tau = T - t. \tag{1.8}$$

Then (1.6), (1.3) becomes

$$\frac{\partial V}{\partial \tau} = \frac{1}{2}\sigma^2 S^2 \frac{\partial^2 V}{\partial S^2} + rS\frac{\partial V}{\partial S} - rV, \qquad S \times \tau \in [0, S_{Max}] \times [0, T], \tag{1.9}$$

$$V(S, T-\tau) = V(S, T-0) = max(E - S, 0), \tag{1.10}$$

which is now a forward parabolic PDE that we are going to investigate into.

1.2 Motivations

Although equation (1.9) is formally parabolic, the numerical approximation behaves as if it was hyperbolic when its convection term plays a dominant role [3]. To describe this phenomenon, the Péclet number (Pe) is defined by the ratio of the convection rate over the diffusion rate in a convection-diffusion transport system [4]. For the case where $Pe >> 1$, we call the PDE a convection-dominated problem. The solution to the convection-dominated problem is usually not so smooth due to the low diffusion term. Since the traditional numerical schemes rely on the smoothness of the solution, spurious oscillations arise when conventional numerical PDE methods are applied.

In financial markets, the convection-dominated problem usually occurs during FX option pricing due to the low asset price and/or low volatilities of the underlying asset [5]. Although the spurious oscillations don't often affect the accuracy of approximated option values, the Greeks such as Delta ($\Delta = \frac{\partial V}{\partial S}$) is corrupted. Then the conventional finite difference method no longer has the advantage of calculating Greeks accurately and efficiently, and the risk control will also be affected because of the inaccurate Greeks. Additionally, the study of this problem will help with the computation of the Black-Scholes equation for Asian options, which is naturally convection-dominated. Therefore, we will explore robust numerical methods for this kind of problem under the Black-Scholes framework.

1.3 Spurious Oscillations in the Numerical Solution of the Convection Dominated B-S Equation

In this subsection, we will demonstrate that spurious oscillations do occur when Péclet number is large and a conventional numerical scheme (the Crank-Nicolson method) is applied.

Assume that the space domain $[0, S_{Max}]$ is divided uniformly into N subintervals. Then the mesh size is $h_S = \frac{S_{Max}}{N}$ and the grid points are $S_i = ih_S$ for $i = 0, 1, 2, \ldots, N$. Similarly, we assume the time domain $[0, T]$ is divided uniformly into M subintervals. So the mesh size is $h_t = \frac{T}{M}$ and the grid points are $\tau_i = ih_t$ for $i = 0, 1, 2, \ldots, N$. Let V_i^j denote the option value when $S = S_i, \tau = \tau_j$.

We approximate $\frac{\partial^2 V}{\partial S^2}|_i$ and $\frac{\partial V}{\partial S}|_i$ using the most usual second order center difference scheme:

$$\frac{\partial^2 V}{\partial S^2}|_{ij} = \frac{V_{i-1}^j - 2V_i^j + V_{i+1}^j}{h_S^2} + \mathcal{O}(h_S^2), \tag{1.11}$$

$$\frac{\partial V}{\partial S}|_{ij} = \frac{V_{i+1}^j - V_{i-1}^j}{2h_S} + \mathcal{O}(h_S^2). \tag{1.12}$$

And the forward Euler method is used to discretize the time space:

$$\frac{\partial V}{\partial \tau}|_{ij} = \frac{V_i^j - V_i^{j-1}}{h_t} + \mathcal{O}(h_t) \tag{1.13}$$

Then from time τ_{j-1} to τ_j, we have θ-time-stepping scheme:

$$\begin{aligned}\frac{V_i^j - V_i^{j-1}}{h_t} &= \theta(\frac{1}{2}\sigma^2 S^2 \frac{V_{i-1}^j - 2V_i^j + V_{i+1}^j}{h_S^2} + rS\frac{V_{i+1}^j - V_{i-1}^j}{2h_S} - rV_i^j) \\ &+ (1-\theta)(\frac{1}{2}\sigma^2 S^2 \frac{V_{i-1}^{j-1} - 2V_i^{j-1} + V_{i+1}^{j-1}}{h_S^2} + rS\frac{V_{i+1}^{j-1} - V_{i-1}^{j-1}}{2h_S} - rV_i^{j-1}).\end{aligned}$$

In (1.3), the parameter $\theta \in [0, 1]$ usually takes the following values, giving rise to different schemes:

- $\theta = 0$: the explicit scheme (conditionally stable, truncation error $\sim \mathcal{O}(h_t + h_S^2)$),
- $\theta = \frac{1}{2}$: the Crank-Nicolson scheme (unconditionally stable, truncation error $\sim \mathcal{O}(h_t^2 + h_S^2)$),
- $\theta = 1$: the implicit scheme (unconditionally stable, truncation error $\sim \mathcal{O}(h_t + h_S^2)$).

The Crank-Nicolson scheme is usually regarded as the best scheme among all three schemes due to its unconditional stability and smaller truncation error. Thus, it's intuitive to apply the C-N scheme to (1.9), and the C-N scheme does give good approximations to (1.9) when the Péclet number is not too large.

However, the approximation is bad when the Péclet number $>> 1$: although the C-N scheme gives approximations with good accuracy and order of convergence (see table 1.1), the existence of spurious oscillations violate the financial rule. For example, negative option value occurs, which is ridiculously incorrect (see figure 1.1, 1.2). Hence, better numerical schemes need to be applied.

With $M = 128$, $\sigma = 0.025$, $r = 0.1$, $S_{Max} = 6$, $E = 1$, $T = 4$ and the C-N scheme,								
N	L^∞ error in V	Order	L^2 error in V	Order	L^∞ error in $\frac{\partial V}{\partial S}$	Order	L^∞ error in $\frac{\partial V}{\partial S}$	Order
16	4.48e-02	N/A	5.63e-03	N/A	4.51e-01	N/A	4.51e-02	N/A
32	2.87e-02	0.64	2.05e-03	1.45	3.86e-01	0.22	2.56e-02	0.82
64	1.60e-02	0.84	1.04e-03	0.98	2.61e-01	0.57	1.19e-02	1.11
128	9.34e-03	0.78	2.92e-04	1.84	2.29e-01	0.19	6.47e-03	0.87
256	3.58e-03	1.38	7.04e-05	2.05	1.09e-01	1.07	2.31e-03	1.49
512	9.63e-04	1.90	1.69e-05	2.06	4.22e-02	1.37	6.07e-04	1.93
1024	2.54e-04	1.92	4.57e-06	1.89	1.21e-02	1.80	1.66e-04	1.87

Table 1.1: L^∞, L^2 errors and their orders of convergence when the Crank-Nicolson scheme is applied

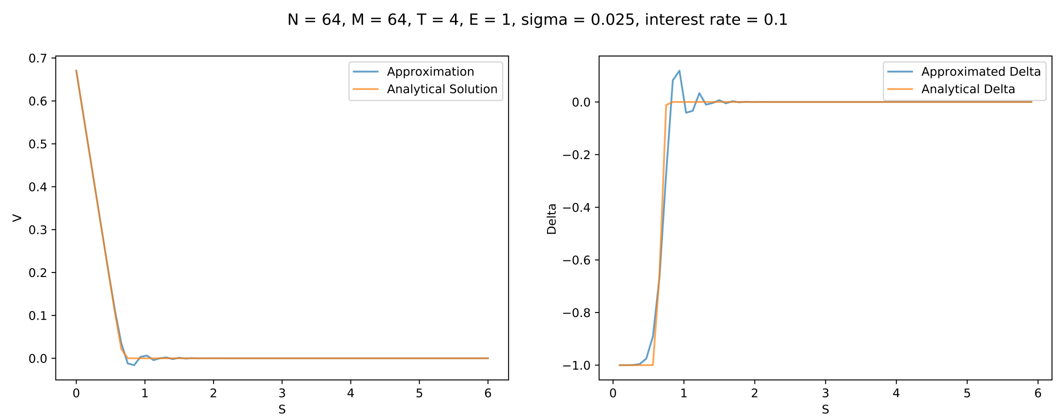

Figure 1.1: Crank-Nicolson scheme: Spurious oscillations example

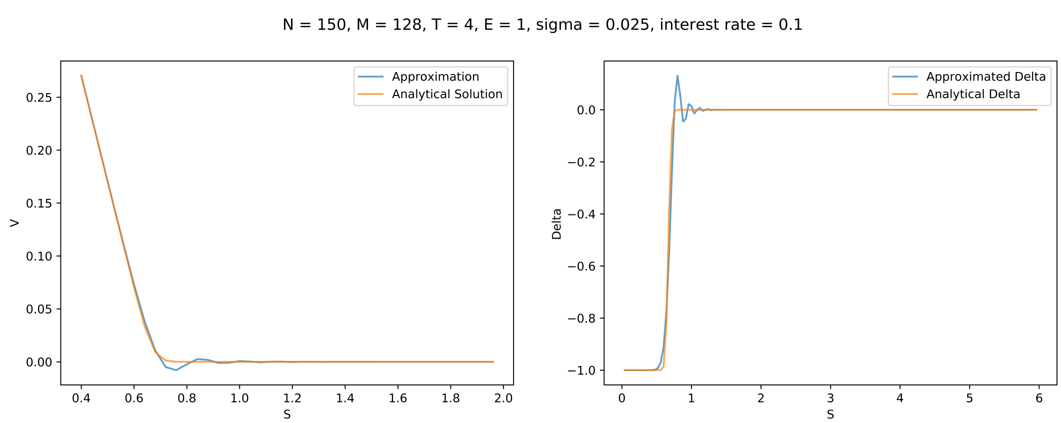

Figure 1.2: Crank-Nicolson: Oscillations still exist even if the space is discretized into 150 subintervals

2 Upwind Scheme

The upwind scheme have become very popular for solving hyperbolic partial differential equations with discontinuous solutions, without the occurrence of spurious oscillations [6]. While upwind techniques can eliminate spurious oscillations, they introduce excessive numerical diffusion and tend to greatly smear the moving steep fronts in these problems [7].

In this chapter, we will show the inaccuracy of the approximation using upwind schemes by numerical experiments, and explore the reason why the numerical diffusion plays a dominated role in this problem.

2.1 Discretization

To illustrate the scheme, we consider the following one-dimensional linear advection equation

$$\frac{\partial u}{\partial t} = a\frac{\partial u}{\partial x} \tag{2.1}$$

where a is a variable that represents the velocity. If a is positive, the solution tends to propagate towards the right, and vice versa.
Define

$$a^+ = max(a, 0), \qquad a^- = min(a, 0) \tag{2.2}$$

and

$$u_x^- = \frac{u_i^n - u_{i-1}^n}{\Delta x}, \qquad u_x^+ = \frac{u_{i+1}^n - u_i^n}{\Delta x} \tag{2.3}$$

Then $a\frac{\partial u}{\partial x}|_i^j$ is approximated by

$$a^- u_x^- + a^+ u_x^+ \tag{2.4}$$

which is called the first-order upwind scheme.
Note that it is stable if the following Courant-Friedrichs-Lewy condition (CFL) is satisfied [8]:

$$c = |\frac{a\Delta t}{\Delta x}| \leq 1, \tag{2.5}$$

which can be easily achieved with any reasonable discretization.

Since in (1.9), the coefficient of $\frac{\partial u}{\partial x}$ is rS, which is always positive in the domain of interest. Then the discretization of (1.9) becomes

$$\begin{aligned} \frac{V_i^j - V_i^{j-1}}{h_t} &= \theta(\frac{1}{2}\sigma^2 S^2 \frac{V_{i-1}^j - 2V_i^j + V_{i+1}^j}{h_S^2} + rS\frac{V_{i+1}^j - V_i^j}{h_S} - rV_i^j) \\ &+ (1-\theta)(\frac{1}{2}\sigma^2 S^2 \frac{V_{i-1}^{j-1} - 2V_i^{j-1} + V_{i+1}^{j-1}}{h_S^2} + rS\frac{V_{i+1}^{j-1} - V_i^{j-1}}{h_S} - rV_i^{j-1}). \end{aligned} \tag{2.6}$$

2.2 Numerical Experiments

Numerical experiments were conducted with the following parameters on an European Put option:

Put Option: $K = 1, T = 4, \sigma = 0.025, r = 0.1$

Grid: $S_{Max} = 6, M = 128$

With $M = 128$, $\sigma = 0.025$, $r = 0.1$, $S_{Max} = 6$, $E = 1$, $T = 4$ and the upwind scheme,								
N	L^∞ error in V	Order	L^2 error in V	Order	L^∞ error in $\frac{\partial V}{\partial S}$	Order	L^∞ error in $\frac{\partial V}{\partial S}$	Order
16	4.60e-02	N/A	4.94e-03	N/A	4.27e-01	N/A	4.55e-02	N/A
32	2.58e-02	0.84	1.88e-03	1.39	3.67e-01	0.22	2.58e-02	0.82
64	3.04e-02	-0.24	9.44e-04	0.99	2.80e-01	0.39	1.13e-02	1.19
128	1.85e-02	0.71	4.30e-04	1.13	2.16e-01	0.37	6.95e-03	0.70
256	1.09e-02	0.77	2.12e-04	1.02	1.51e-01	0.52	3.94e-03	0.82
512	6.26e-03	0.79	1.07e-04	0.99	9.39e-02	0.69	2.15e-03	0.88
1024	3.41e-03	0.88	5.36e-05	0.99	5.71e-02	0.72	1.16e-03	0.90

Table 2.1: The Upwind Scheme: L^∞, L^2 errors and their orders of convergence.

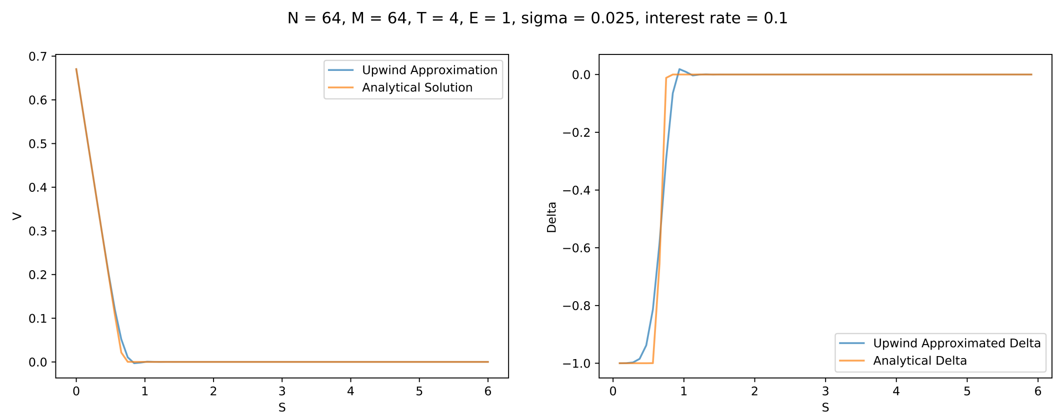

Figure 2.1: The Upwind Scheme: Oscillations disappeared.

From the results 2.1 and 2.1, we can see that although the spurious oscillations disappeared, the accuracy of the approximation is worse than the one produced by C-N scheme once the space domain is discretized into more than ~32 subintervals. This is because the upwind scheme's order of convergence with respect to space domain is $\mathcal{O}(h_S)$, which is less than the one of the Crank-Nicolson method ($\mathcal{O}(h_S^2)$).

2.3 The Flaw Behind the Upwind Scheme: Numerical Diffusion

First we show that the upwind scheme adds numerical diffusion terms into our PDE (1.9), which smooths the solution out. By Taylor expansion,

$$\frac{V_{i+1}^j - V_i^j}{h_S} = \frac{V_i^j + h_S \frac{\partial V}{\partial S}|_i^j + \frac{h_S^2}{2}\frac{\partial^2 V}{\partial S^2}|_i^j + \mathcal{O}(h_S^3) - V_i^j}{h_S} = (\frac{\partial V}{\partial S} + \frac{h_S}{2}\frac{\partial^2 V}{\partial S^2})|_i^j + \mathcal{O}(h_S^2). \tag{2.7}$$

Up to a second-order truncation error, we can re-written the original Black-Schole equation (1.9) as

$$\frac{\partial V}{\partial \tau} = \frac{1}{2}\sigma^2 S^2 \frac{\partial^2 V}{\partial S^2} + rS(\frac{\partial V}{\partial S} + \frac{h_S}{2}\frac{\partial^2 V}{\partial S^2}) - rV \tag{2.8}$$

or

$$\frac{\partial V}{\partial \tau} = \frac{1}{2}(\sigma^2 S^2 + rSh_S)\frac{\partial^2 V}{\partial S^2} + rS\frac{\partial V}{\partial S} - rV \tag{2.9}$$

Notice that the spurious oscillations and/or inaccurate approximations happen only when the stock price is close to the strike price, which equals 1 in our previous numerical experiments. Therefore, we set $S \approx 1$ in our following analysis.

The coefficient of the diffusion term in the original Black-Scholes equation is $\frac{1}{2}\sigma^2 S^2 \approx \frac{1}{2}\sigma^2$. And the coefficient of the numerical diffusion term is $\frac{1}{2}rSh_S \approx \frac{1}{2}rh_S$. Since σ and r are set to be 0.01 and 0.08 respectively in our numerical experiments, we are able to compute the ratio of the coefficient of numerical diffusion term over the coefficient of exact diffusion term. See table 2.2.

h_S	$S_{Max}/16$	$S_{Max}/32$	$S_{Max}/64$	$S_{Max}/128$	$S_{Max}/256$	$S_{Max}/512$	$S_{Max}/1024$
Coefficient of the numerical diffusion term	3.00e-02	1.50e-02	7.50e-03	3.75e-03	1.87e-03	9.37e-04	4.69e-04
Ratio	3.33e+01	1.67e+01	8.33e+00	4.17e+00	2.08e+00	1.04e+00	5.21e-01

Table 2.2: the ratio of the coefficient of numerical diffusion term over the coefficient of exact diffusion term.

Notice that the effect of the numerical diffusion is still 4% larger than the effect of exact diffusion even if we discretize the space domain into 512 subintervals, i.e., the numerical diffusion plays a dominant role for any reasonable space discretization sizes. This explains the reason why the elimination of the spurious oscillation doesn't guarantee us a more accurate result.

3 Total Variation Diminishing Scheme with van Leer Flux Limiter

In the previous two chapters, we illustrated that both the Crank-Nicolson scheme and the upwind scheme have their strengths and weaknesses: the Crank-Nicolson scheme has a higher order of accuracy, but the spurious oscillations produce unaccepted phenomena, such as negative option values; the upwind scheme eliminates the oscillations by introducing numerical diffusion, causing the approximation to be inaccurate. Thus, both methods are not ideal.

In this chapter, we are going to introduce a finite volume discretization approach that gives accurate results without producing spurious oscillations.

3.1 Finite Volume Discretization of the Black-Scholes Equation

A finite volume discretization of 1D convection-diffusion-reaction equation is given in [3]:

$$\frac{V_i^n - V_i^{n-1}}{h_t} + \theta(F_{i+1/2}^n - F_{i-1/2}^n + f_i^n) + (1-\theta)(F_{i+1/2}^{n-1} - F_{i-1/2}^{n-1} + f_i^{n-1}) = 0 \tag{3.1}$$

where

$$\theta = \text{temporal weighting } (0 \leq \theta \leq 1) \tag{3.2}$$

$$F_{i-1/2} = \text{flux entering cell i at interface } i - 1/2 \tag{3.3}$$

$$F_{i+1/2} = \text{flux leaving cell } i \text{ at interface } i + 1/2 \tag{3.4}$$

$$f_i = \text{source/sink term.} \tag{3.5}$$

In particular, the flux and the source/sink terms are defined by

$$F^n_{i\pm1/2} = \frac{1}{h_x}\bigg(\mp \frac{1}{2}\sigma^2 S_i^2 \frac{V_{i\pm1} - V_i^n}{h_x} - rS_i V^n_{i\pm1/2}\bigg), \tag{3.6}$$

$$f_i^n = rV_i^n. \tag{3.7}$$

So all we need is to approximate the value of $V^n_{i\pm1/2}$, such that we can get a linear system to solve.

The crudest way to use the central weighting scheme

$$V^n_{i\pm1/2} = \frac{V^n_{i\pm1} + V^n_i}{2}, \tag{3.8}$$

which is equivalent to discretize the $\frac{\partial V}{\partial S}$ term using the center difference scheme. We have already illustrated that it will lead to spurious oscillations in section 1.3. Therefore, we have to seek for a more sophisticated approximation.

3.2 Total Variation Diminishing Scheme

To measure the level of severity of spurious oscillations, we introduce the concept of Total Variance (TV), defined by

$$TV = \sum_{j=0}^{N-1} |V_{j+1} - V_j|. \tag{3.9}$$

A numerical scheme is called *total variation diminishing (TVD)* if $TV^{(n+1)} \leq TV^{(n)}$. This inequality will eliminate the occurrence of spurious oscillations, due to the fact that oscillations naturally cause the total variance to increase.

Since the coefficient of the diffusion term in (1.9) is always positive throughout the simulation, $V^n_{i\pm1/2}$ can be approximated by the following total variation diminishing scheme [7]:

$$V^{n-1}_{i+1/2} = V^{n-1}_{i+1} + \frac{1}{2}\Psi(\frac{V^{n-1}_{i+1} - V^{n-1}_{i+2}}{V^{n-1}_i - V^{n-1}_{i+1}})(V^{n-1}_i - V^{n-1}_{i+1}), \tag{3.10}$$

where $\Psi(q)$ is a flux limiter, and $\frac{V^{n-1}_{i+1} - V^{n-1}_{i+2}}{V^{n-1}_i - V^{n-1}_{i+1}}$ represents the ratio of successive gradients on the solution mesh.

The existence of the flux limiter is to assure that numerical diffusion is added only at points where the solution has steep gradient [7], which guarantees an accurate approximation without spurious oscillations. A good choice of the limiter function Ψ will be the van Leer flux limiter, which is defined by

$$\Psi(r) = \frac{r + |r|}{1 + |r|}. \tag{3.11}$$

We can see from the figure 3.1 that the point $(1, 1)$ is the fixed point of the function, i.e., this limiter function tends to make the input closer to 1 in order to smooth the approximation.

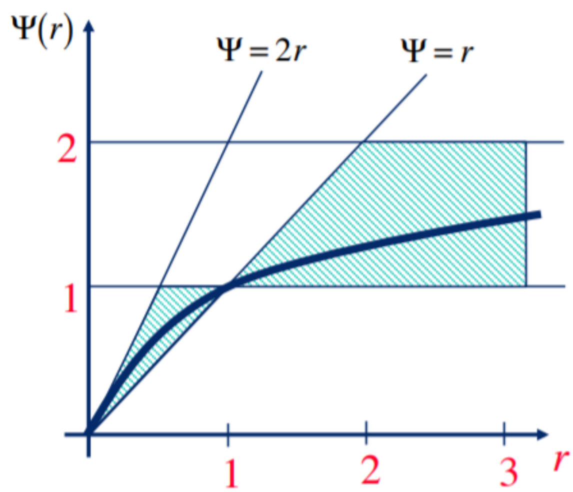

Figure 3.1: van Leer limiter function overlaid onto second-order TVD region [9].

3.3 Numerical Experiments

Numerical experiments in the table 3.1 were conducted with the following parameters on an European Put option:

$$\text{Put Option: } K = 1, T = 4, \sigma = 0.025, r = 0.1$$

$$\text{Grid: } S_{Max} = 6, M = 128$$

Notice that this scheme eliminates the spurious oscillations arisen from the convection-dominated B-S equation.

With $M = 128$, $\sigma = 0.025$, $r = 0.1$, $S_{Max} = 6$, $E = 1$, $T = 4$ and the TVD scheme,								
N	L^∞ error in V	Order	L^2 error in V	Order	L^∞ error in $\frac{\partial V}{\partial S}$	Order	L^∞ error in $\frac{\partial V}{\partial S}$	Order
16	4.20e-02	N/A	3.17e-03	N/A	3.66e-01	N/A	3.90e-02	N/A
32	1.90e-02	1.14	9.61e-04	1.72	2.90e-01	0.34	2.07e-02	0.91
64	1.28e-02	0.57	5.58e-04	0.78	1.66e-01	0.80	9.39e-03	1.14
128	5.82e-03	1.14	1.85e-04	1.60	1.46e-01	0.18	4.50e-03	1.06
256	2.20e-03	1.41	4.99e-05	1.89	8.15e-02	0.85	1.59e-03	1.50
512	5.60e-04	1.97	1.11e-05	2.17	2.70e-02	1.59	3.93e-04	2.02
1024	1.10e-04	2.34	2.09e-06	2.41	5.34e-03	2.34	7.44e-05	2.40

Table 3.1: The TVD Scheme: L^∞, L^2 errors and their orders of convergence.

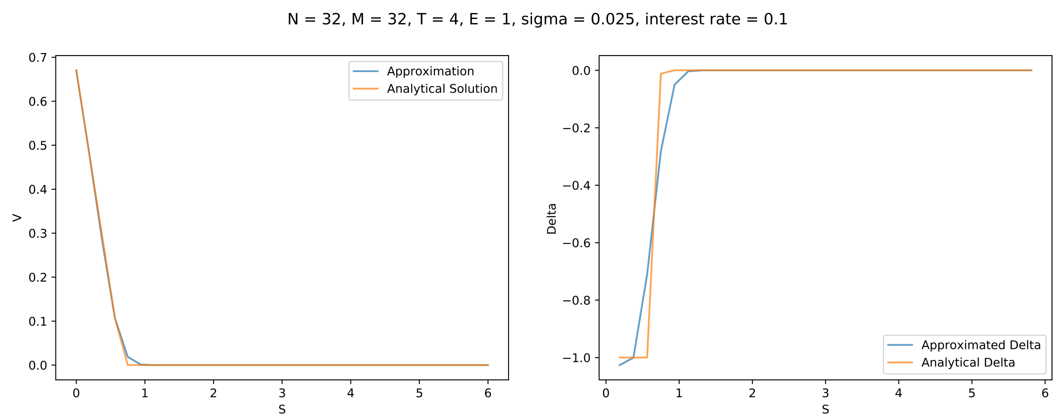

Figure 3.2: Spurious oscillations don't occur when the space is only discretized into 32 subintervals.

Moreover, with the same amount of subintervals in space and time, its numerical error in V and $Delta$ is less than the one of the Crank-Nicolson scheme.

In the figure 3.3, we contrast the accuracy of the C-N, upwind and TVD schemes with respect to error in V and Δ. Note that the accuracy of the upwind scheme is similar to the one of the Crank-Nicolson scheme when the space domain is discretized into less than ~ 100 subintervals, since the numerical dispersion of C-N scheme and the upwind scheme's first order of accuracy cancel each other out. In this case, the upwind scheme is favored since the oscillation-free approximation given by it satisfy the financial rule more. However, after the meshes get finer, the Crank-Nicolson scheme is better due to its higher order of accuracy.

It's obvious that the TVD scheme outweighs the other two schemes due to its good order of accuracy and free of spurious oscillations. Therefore, we believe the TVD scheme with van-Leer flux limiter is a better method for the Black-Scholes equation when the market volatility is small.

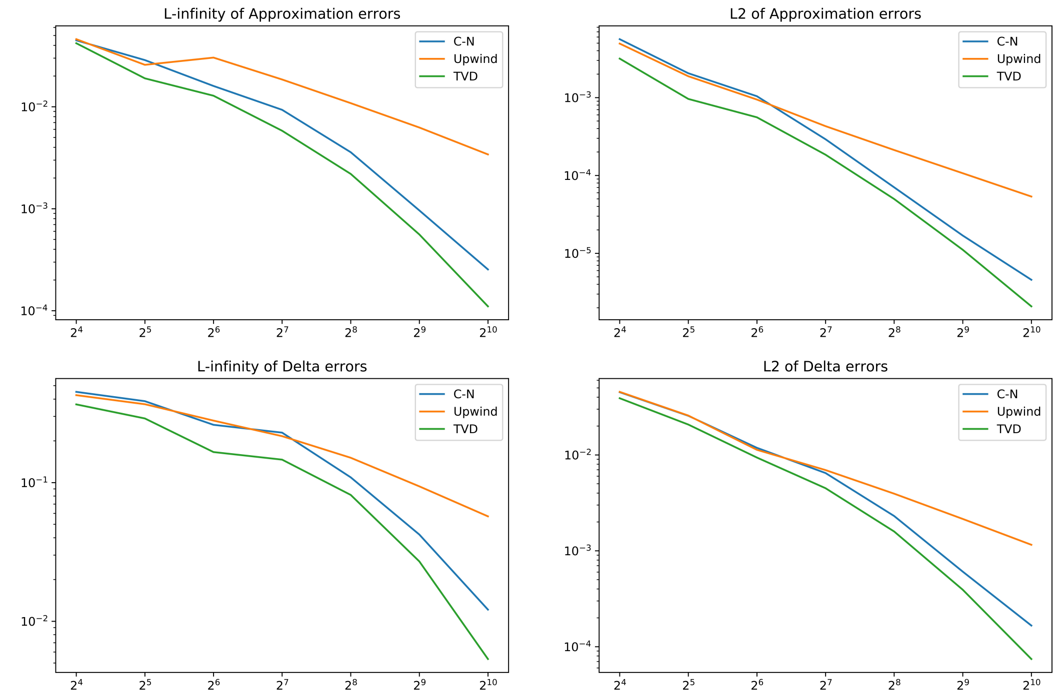

Figure 3.3: A comparison of approximations produced by the C-N, the upwind and the TVD scheme.

4 Further Study: Discontinuous Galerkin Method

The discontinuous Galerkin method is the modern FEM approach for solving PDEs, with which we can easily introduce higher-order scheme. Additionally, it's free of oscillations. The main difference between the DG method and the usual FEM method lies in the choice of basis: In the DG method, we don't enforce any continuity constraints between elements. See figure 4.1 and 4.2. Here we introduce the formulation of the DG approach to the B-S equation 1.9.

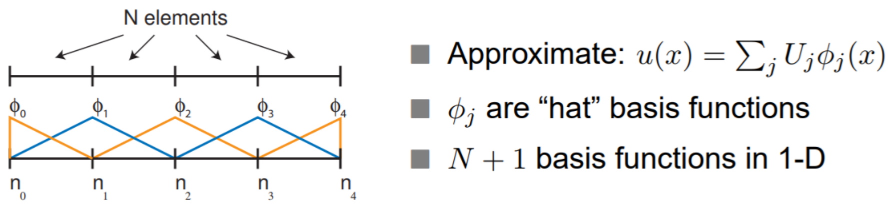

Figure 4.1: Usual FEM basis functions [10].

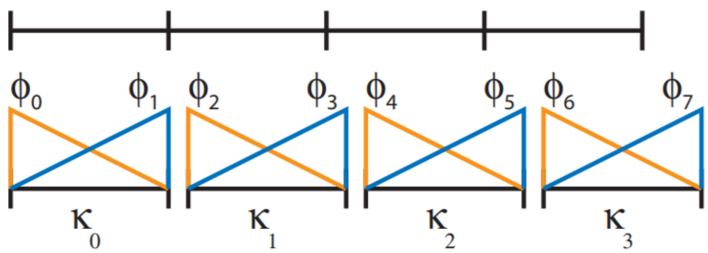

Figure 4.2: Usual discontinuous Galerkin method basis functions [10].

For an element $[a, b]$, we define the basis to be

$$\phi_0(S) = \frac{1}{b-a}S - \frac{a}{b-a}, \tag{4.1}$$

$$\phi_1(S) = \frac{1}{a-b}S - \frac{b}{a-b}. \tag{4.2}$$

Note that in the usual DG approach, people prefer to use higher-order basis functions. However, the linear basis functions will work well in our case since the solution to convection-dominated B-S equation is close to a hockey stick function.

Then we introduce the weak form of the PDE. Assume that $V(t,x) = \sum_{i=0}^{1} a_i(t)\phi_i(x)$. For generality, we define $\Omega = [a, b]$. For $j = 0, 1$,

$$\int_\Omega \frac{\partial V}{\partial \tau}\phi_j dS - \frac{\sigma^2}{2}\int_\Omega S^2\frac{\partial^2 V}{\partial S^2}\phi_j dS - r\int_\Omega S\frac{\partial V}{\partial S}\phi_j dS + r\int_\Omega V\phi_j dS = 0. \tag{4.3}$$

We apply integration by parts to reduce the requirements of the smoothness of V, which gives us

$$\int_\Omega \frac{\partial V}{\partial \tau}\phi_j dS = \sum_{i=0}^{1} a_i'(t)\int_\Omega \phi_i\phi_j dS, \tag{4.4}$$

$$-\frac{\sigma^2}{2}\int_\Omega S^2\frac{\partial^2 V}{\partial S^2}\phi_j dS = -\frac{\sigma^2}{2}\left([(\sum_{i=0}^{1}a_i(t)\phi_i'(x))S^2\phi_j]_a^b - \int_\Omega(\sum_{i=0}^{1}a_i(t)\phi_i(x))(2S\phi_j + S^2\phi_j')dS\right), \tag{4.5}$$

$$-r\int_\Omega S\frac{\partial V}{\partial S}\phi_j dS = -r\left([(\sum_{i}^{1}a_i(t)\phi_i(x))S\phi_j]_a^b - \int_\Omega(\sum_{i=0}^{1}a_i(t)\phi_i(x))(\phi_j + S\phi_j')dS\right), \tag{4.6}$$

$$r\int_\Omega V\phi_j dS = r\int_\Omega(\sum_{i=0}^{1}a_i(t)\phi_i(x))\phi_j dS. \tag{4.7}$$

By plugging the four equations back into (4.3) and writing them in the matrix form, we will get

$$Ma' - (\frac{\sigma^2}{2}K + rL - rM)a = 0 \tag{4.8}$$

or

$$Ma' = (\frac{\sigma^2}{2}K + rL - rM)a. \tag{4.9}$$

For each time step, we have a, which means that we can compute a' by solving the linear system. Then we can compute the a at the next time step by the Forward Euler method, i.e.,

$$a^{(n)} = a^{(n-1)} + a'h_t. \tag{4.10}$$

Note that the CFL condition needs to be satisfied to make the scheme stable.

5 Summary

In equity and FX option markets, due to the low asset prices and/or low volatilities, the Black-Scholes equation becomes convection-dominated [5], leading to spurious oscillations in our numerical approximations. Although we have the analytical solution to the original Black-Scholes equation, it may not be the case when more sophisticated conditions such as jump-diffusion models, local volatility are assumed. Additionally, the Asian option model and one-factor interest rate models of the Vasicek type are usually convection-dominated for typical market data. Therefore, it's meaningful to study this kind of problem in the original B-S model first.

In Chapter 1, we introduced the reader into the definition of the Black-Scholes equation, mentioning the conventional discretization of the parabolic PDE: the Crank-Nicolson scheme. Then we considered a case where the Péclet of the problem is large. Because of the severe numerical dispersion of the Crank-Nicolson scheme, the numerical experiments show the existence of spurious oscillations.

The next chapter was dedicated to proving that the first-order upwind scheme is unable to handle the problem. Although the upwind scheme gives an oscillation-free result, the numerical diffusion that it introduced severely increases the coefficient of the diffusion term, making the approximation inaccurate. Thus, a better method needs to be proposed.

In the third chapter, we discretized the Black-Scholes equation using the finite volume approach, which enables us to apply the total variation diminishing scheme with flux limiters. Since this scheme guarantees that the total variation is decreasing, oscillations naturally disappeared. By the selection of our flux limiter, the scheme is of the second order of accuracy. We showed that it is the most favoured scheme for the problem by numerical experiments.

Finally, we introduced the *discontinuous Galerkin method* for the further study of the convection-dominated problem.

References

[1] F. Black and M. Scholes. The pricing of options and corporate liabilities. pages 637–654, 1973.

[2] P. Wilmott, S. Howison, and J. Dewynne. *The Mathematics of Financial Derivatives*. Cambridge University Press, 1995.

[3] R. Zvan, P.A. Forsyth, and K. Vetzal. Robust numerical methods for pde models of asian options. volume 1, 1997.

[4] T. L. Bergman, A. S. Lavine, F. P. Incropera, and D. P. DeWitt. *Fundamentals of Heat and Mass Transfer*. Wiley: New York, 2011.

[5] J. Topper. *Financial Engineering with Finite Elements*. Wiley, 2005.

[6] M. Brio and C. C. Wu. An upwind differencing scheme for the equations of ideal magnetohydrodynamics. pages 400–422, 1988.

[7] Z. Wang, M. A. Lawatia, and H. Wang. An eulerian-lagrangian method for option pricing in finance. volume 23, 2007.

[8] R. Courant, K. Friedrichs, and H. Lewy. On the partial difference equations of mathematical physics. volume 11, 1967.

[9] B. Seibold. *Numerical Methods for Partial Differential Equations*. MIT 18.336, 2009.

[10] K. J. Fidkowski. *An Introduction to the Discontinuous Galerkin Method*. University of Michigan, 2005.